the plant journal

SEB SOCIETY FOR EXPERIMENTAL BIOLOGY

The Plant Journal (2009) **58**, 109–121 doi: 10.1111/j.1365-313X.2008.03764.x

BTB and TAZ domain scaffold proteins perform a crucial function in *Arabidopsis* development

Hélène S. Robert†, Ab Quint, Daan Brand, Adam Vivian-Smith and Remko Offringa*

Department of Molecular and Developmental Genetics, Institute of Biology, Leiden University, Wassenaarseweg 64, 2333 AL Leiden, The Netherlands

Received 18 July 2008; revised 17 November 2008; accepted 20 November 2008; published online 5 January 2009.
*For correspondence (fax +31 71 5274999; e-mail r.offringa@biology.leidenuniv.nl).
†Present address: Department of Plant Systems Biology, VIB, Ghent University, Technologiepark 927, 9052 Ghent, Belgium.

Summary

In *Arabidopsis*, bric-a-brac, tramtrack and broad (BTB) domain scaffold proteins form a family of 80 proteins that have involvement in various signaling pathways. The five members of the subfamily of BTB AND TAZ DOMAIN proteins (BT1–BT5) have a typical domain structure that is only observed in land plants. Here, we present a functional analysis of the BT family, of which at least four members are encoded by auxin-responsive genes. BT1 is a short-lived protein that is characteristically targeted for degradation by the 26S proteasome. Expression pattern, gene structure and sequence analyses indicate that BT1 and BT2 are closely related. They both localize to the nucleus and the cytosol, whereas the remaining BT proteins were determined as cytosolic proteins. Detailed molecular and phenotypic analysis of plants segregating for null mutations in the *BT* family revealed substantial redundancy among the *BT* members, and highlighted that BT proteins perform crucial roles in both male and female gametophyte development. *BT2* seems to be the predominant gene in this process, in which it is functionally replaced by *BT3* and *BT1* through reciprocal transcription regulation. Compensational expression alters the steady-state mRNA levels among the remaining *BT* family members when other *BT* members are lost, and this contributes towards functional redundancy. Our data provide a surprising example of functional redundancy among genes required during gametophyte development, something that could not be detected in the current screens for gametophyte mutants.

Keywords: gametophyte development, functional redundancy, reciprocal transcription regulation, protein–protein interaction domain, auxin responsive, 26S proteasome.

Introduction

Effector proteins in basic cellular processes act generally as part of a protein complex that is held together by one or more scaffold or linker proteins. The importance of scaffold proteins has for a long time been undervalued, but the finding that loss of function leads to lethality, for instance for CULLIN1 and CULLIN3 (CUL3) that are induced in targeted proteolysis (Hellmann *et al.*, 2003; Gingerich *et al.*, 2005), has revealed their underlying importance, and has revived the interest in scaffolding processes.

Scaffold proteins are characterized by their protein–protein interaction domains, which are conserved and form the basis of their classification. One of the largest families of scaffold proteins is formed by so-called bric-a-brac, tramtrack and broad (BTB) domain proteins. The conserved BTB domain was first identified in *Drosophila melanogaster* proteins, which are central components of the BTB protein complexes of transcriptional regulators. It is also referred to as the POZ domain because of its occurrence in many pox virus zinc-finger proteins (Albagli *et al.*, 1995). Currently, BTB proteins have been identified in many other eukaryotes, including yeasts, *Caenorhabditis elegans*, mammals and plants (Bardwell and Treisman, 1994; Stogios *et al.*, 2005).

The genomes of the model plants Arabidopsis and rice encode, respectively, 80 and 149 BTB proteins classified in 10 subfamilies (Gingerich *et al.*, 2005, 2007), of which only a few have been studied in detail. Most, but not all, Arabidopsis BTB proteins combine the BTB domain with at least one other protein–protein interaction domain that appears

to assign a specific cellular function to these proteins. For example, the ankyrin and armadillo domains that are found in other BTB proteins are involved in transcriptional regulation (Cao *et al.*, 1997; Ha *et al.*, 2004; Hepworth *et al.*, 2005; Norberg *et al.*, 2005), whereas the MATH and TPR domain-containing BTB proteins BTB/POZ-MATH, ETHYLENE OVERPRODUCER 1 (ETO1) and ETO1-like proteins EOL1 and EOL2 each form an E3 ubiquitin protein ligase complex with CUL3, which labels proteins for degradation by the 26S proteasome (Wang *et al.*, 2004; Dieterle *et al.*, 2005; Gingerich *et al.*, 2005; Weber *et al.*, 2005). Other plant BTB proteins take part in a variety of cellular processes, such as phototropic responses for NPH3 (Motchoulski and Liscum, 1999), leaf and flower morphogenesis for BLADE-ON-PETIOLE 1 and 2 (Ha *et al.*, 2004; Hepworth *et al.*, 2005; Norberg *et al.*, 2005), and in ethylene responses for ETO1, EOL1 and EOL2 (Wang *et al.*, 2004).

We identified the BTB AND TAZ DOMAIN (BT) proteins as interacting partners of the protein kinase PINOID (HR, MKZ, RB & RO, unpublished data). The Arabidopsis genome encodes a small subfamily of five BT proteins that consist of an N-terminal BTB domain, a transcriptional adapter zinc finger (TAZ) domain and a C-terminal calmodulin binding (CaMB) domain. Previously, BT proteins were found to interact with the potato calmodulin 6 in a calcium-dependent manner, and BT1, 2 and 4 were found to bind to bromodomain transcriptional regulators (Du and Poovaiah, 2004). Furthermore, BT2 seems to be part of a feedback loop that enhances specific responses to exogenous auxin (Ren *et al.*, 2007). Other than that, not much is known about the function of BT proteins in plant development. Here, we present a functional analysis of the BT family in Arabidopsis. We show that there is functional redundancy among the family members, and that the expression of specific *BT* genes is up- or downregulated when null mutations occur in other *BT* genes. BT proteins are either nuclear and cytoplasmic or only cytoplasmic. Significantly, plants containing multiple null mutations in the different *BT* genes show that BT proteins play an essential role during gametogenesis, and probably throughout plant development.

Results

BT proteins are land-plant specific

A comparison of the five members of the Arabidopsis *BT* family based on amino acid sequence identity of the encoded proteins distinguishes two groups: the first consisting of BT1 and BT2, and the second of BT3, BT4 and BT5 (Figure 1a) (Du and Poovaiah, 2004). This is reflected in the predicted nuclear localization signals (NLSs) and leucine-rich nuclear export signals (NESs) (La Cour *et al.*, 2004) (Figure 1b), present in BT1 and BT2, but not in BT3, BT4 or BT5, and partially in the exon/intron gene structure. Apart from Arabidopsis, BT proteins can be found in rice (Gingerich *et al.*, 2007), Solanaceae (SOL genomic network, http://www.sgn.cornell.edu), *Medicago*, red clover and *Physcomitrella*, but not in algae, yeast, fungi or animals (http://www.ncbi.nlm.nih.gov/Genomes), indicating that the domain structure of the BT family is restricted to land plants (Figure 1a).

In order to investigate the possible function of these proteins in Arabidopsis, lines with T-DNA or transposon insertions in the corresponding genes were obtained from available collections. In each case, the null mutation status of the disrupted gene was verified (Figure 1b–g). All homozygous insertion mutants were indistinguishable from the wild type. These results suggest that *BT* family members perform a non-essential function, or alternatively that functional redundancy exists among *BT* family members in Arabidopsis.

Subcellular localization of BT proteins

A previous analysis of the subcellular localization of BT1 indicated that the protein is predominantly nuclear (Du and Poovaiah, 2004). Indeed, transfection of Arabidopsis protoplasts with *35S::BT1:YFP* showed that BT1:YFP is both nuclear and cytosolic in 62% of the protoplasts (n = 34, Figure 2b), whereas it is cytoplasmic in 38% of the protoplasts (n = 21, Figure 2a). When the C-terminal YFP fusion for BT2 was expressed in protoplasts, 90% (n = 31) of the cells showed cytoplasmic localization (Figure 2c), and 10% of the cells showed both nuclear and cytosolic localization (Figure 2d). The less predominant nuclear localization of BT2 compared with BT1 is in agreement with the ratio of the predicted NLSs and NESs, which is 3:1 in the case of BT1, and 2:2 in the case of BT2 (Figure 1b), and thereby suggests that these putative NLSs and NESs in BT1 and BT2 are functional. BT4:YFP and BT5:YFP were only found in the cytoplasm (n = 40 and 33, respectively; Figures 2e–f), corresponding to the fact that no NLSs were predicted in BT4 and BT5. Western blot analysis confirmed that the protoplast-expressed BT:YFP fusion proteins were full length (Figure 2h).

BT1 is a short-lived protein in Arabidopsis

To confirm the subcellular localization *in planta*, and to further analyze the function of BT proteins, we generated stable transformants using both *35S::BT1:GFP* and *35S::GFP:BT1* constructs, or a construct containing a C-terminal fusion of the BTB domain of BT1 with GFP (*35S::BTB:GFP*). For each construct, at least 25 independent T_2 lines were generated and studied. Each line showed a wild-type phenotype. None of the *35S::BT1:GFP* or *35S::BTB:GFP* lines, and only few of the *35S::GFP:BT1* lines, showed a clear cytosolic fluorescent signal in the root

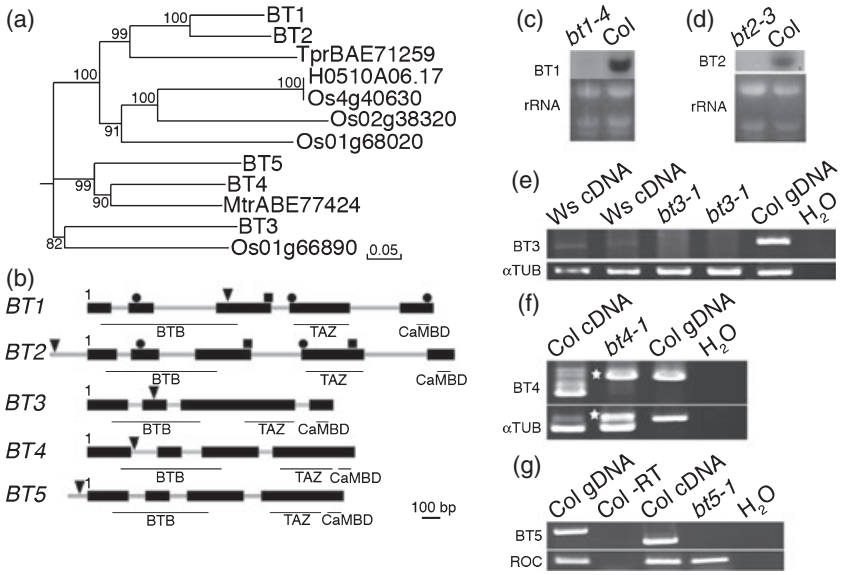

Figure 1. The Arabidopsis *BT* family.

(a) A tree based on the CLUSTALW protein alignment showing the relationship between BT proteins from Arabidopsis, Rice, *Medicago truncatula* and *Trifolium pratense*. The tree is constructed using the neighbor-joining method with a bootstrap test of 10 000 iterations.

(b) The structure of the five Arabidopsis *BT* genes. The black boxes represent the exons. The parts encoding the N-terminal BTB domain, the TAZ domain and the C-terminal CaMBD are underlined. Predicted nuclear localization signals (NLSs) and nuclear export signals (NESs) are indicated by circles and squares, respectively. For *BT1*, three NLSs and one NES are found at positions aa57–60, aa193–203, aa342–345 and aa181–183, respectively. For *BT2*, two NLSs and two NESs are found at positions aa65–81, aa203–212 and aa191–197, aa294–302, respectively. The black arrowhead indicates the position of the T-DNA or transposon insertion in *bt1-4* (GT2847), *bt2-3* (SALK_084471), *bt3-1* (Flag_396E01), *bt4-1* (SALK_045370) and *bt5-1* (GABI-Kat 771C08) at positions +748 bp, –173 bp, +357 bp, +430 bp and –42 bp, respectively, relative to the ATG.

(c–g) Validation of the null allele status of *bt* mutants by northern blot (c, d) and RT-PCR (e–g) analyses in 8-day-old seedlings of *bt1-4* (c), *bt2-3* (d), *bt3-1* (e), *bt4-1* (f) and *bt5-1* (g). Positive controls for the RT-PCR are either the Col-0 or Ws cDNA and genomic DNA (gDNA). Negative controls are reactions in which the RT enzyme was omitted (Col –RT) and water (H_2O). rRNA, α-tubulin and ROC expression were used as loading controls. Note that for the *bt4-1* sample (f; asterisks), genomic DNA contamination was present and the cDNA was absent.

(Figure 2i), resembling that of soluble GFP (Figure 2j). Further analysis demonstrated that no full-length fusion protein could be detected in these GFP positive lines, even though a full-length *GFP:BT1* mRNA was produced *in vivo* (Figure 2k–l). The above result, together with the lack of fluorescent signal in all lines carrying the C-terminal fusion (Figure 2m), suggested to us that BT1 and the BT1:GFP fusions were unstable. To test this, seedlings expressing *BT1:GFP* or *BTB:GFP* were treated with the 26S proteasome inhibitor MG132 (50 μM). After 4 h of treatment, a fluorescent signal was observed both in the nucleus and the cytoplasm of root cells of different lines (Figure 2n–p). Under higher magnification, the nuclear localization was not uniform, but instead consisted of bright dots (Figure 2p). Similar observations have been made for other proteins that are targeted to the 26S proteasome (Hamann *et al.*, 2002; Tao *et al.*, 2005). Western blot analysis confirmed the presence of the full-length fusion proteins, which were significantly more abundant in the MG132-treated samples (Figure 2q). Different treatments with auxin or auxin transport inhibitors did not influence the stability, nor the subcellular localization of the BT1:GFP or BTB:GFP fusion proteins, in the MG132-treated samples. Fluorescent microscopy on tissues other than the root, such as leaves and inflorescences, did not identify tissue-specific stabilization of the BT1:GFP or BTB:GFP fusion proteins (data not shown). These *in planta* results indicate that BT1 is a short-lived nuclear-cytoplasmic protein that is targeted for degradation by the 26S proteasome pathway, and suggest that its proteasome-mediated degradation is linked to the N-terminal BTB domain-containing part of the protein.

Compensational expression among BT *family members*

To examine gene redundancy among *BT* family members, we investigated their expression in different tissues in the wild type and in specific *bt* null mutant backgrounds by northern blot analysis and quantitative RT-PCR (qPCR; Figures S1 and S3a, c and d). The four Arabidopsis *BT* genes analyzed are most abundantly expressed in wild-type rosette leaves. *BT1* and *BT5* are also expressed in stems, whereas *BT2* and *BT5* show significant expression in seedlings, and *BT4* and *BT5* are most abundant in flowers and siliques. In general, these data correlate well with previously published northern and microarray analyses (Figure S2a and b) (Du and Poovaiah, 2004; Zimmermann *et al.*, 2004; Gingerich

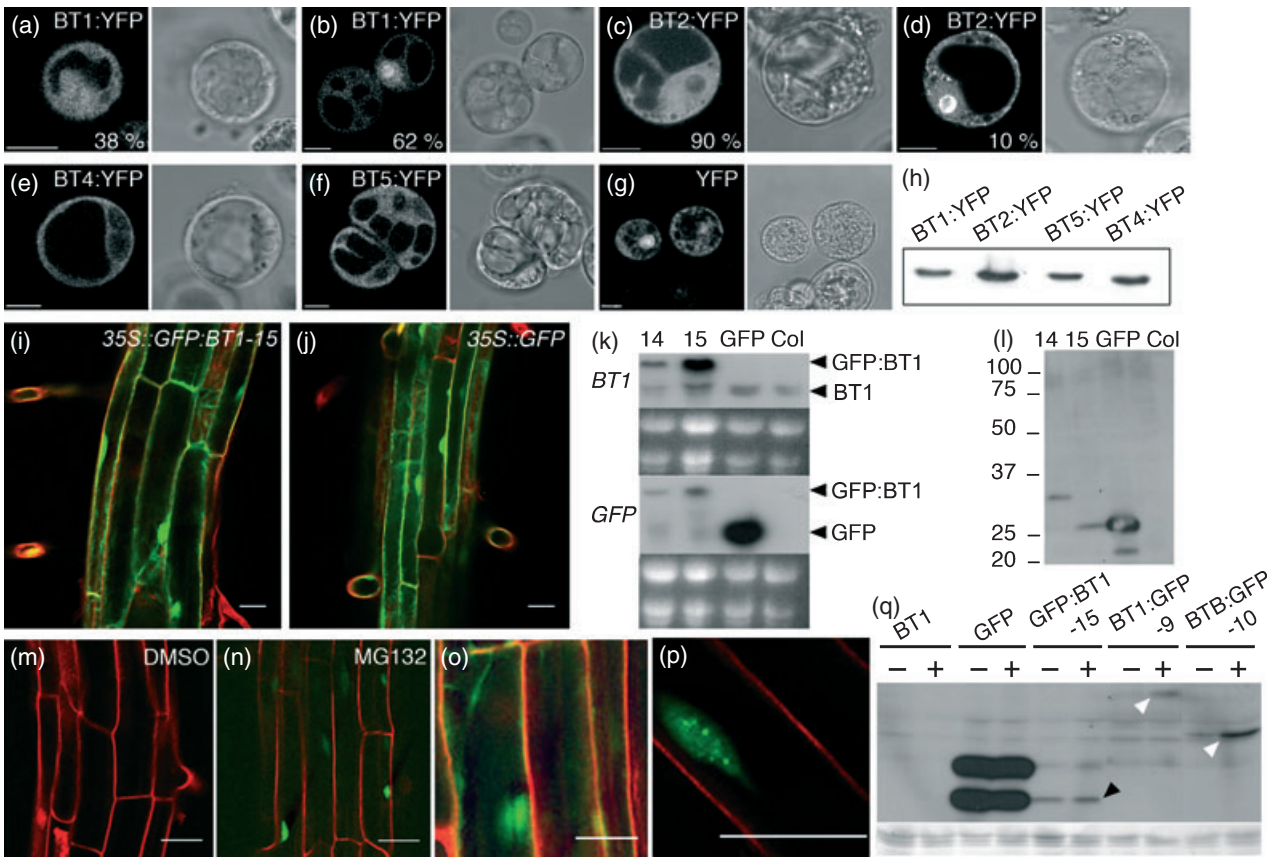

Figure 2. Subcellular localization of Arabidopsis BT proteins.
(a–g) Confocal fluorescent images (left) and the corresponding transmitted light images (right) of Arabidopsis protoplasts expressing C-terminal YFP:HA fusions of BT1 (a, b), BT2 (c, d), BT4 (e) and BT5 (f), or YFP:HA alone (g). For BT1:YFP and BT2:YFP, the percentage of cells showing cytoplasmic (a, c) or both cytoplasmic and nuclear localization (b, d) is indicated.
(h) Western blot analysis of cell extracts with anti-HA confirms the expression of full-length BT:YFP fusion proteins in (a–f).
(i, j) Confocal images of root epidermal cells of the lines *35S::GFP:BT1-15* (i) and *35S::GFP* (j) show identical cytoplasmic and nuclear localized GFP signals.
(k) Northern blot analysis with the *BT1* (top) or the *GFP* probe (bottom) shows that a full-length *GFP:BT1* mRNA is produced in *35S::GFP:BT1* lines 14 and 15.
(l) Western blot probed with anti-GFP antibodies detecting a partial GFP:BT1 fusion (30 kDa) or unfused GFP (27 kDa; GFP:BT1 is 69 kDa) in lines *35S::GFP:BT1-14* and *35S::GFP:BT1-15*, respectively.
(m–p) BT1:GFP is detected in line *35S::BT1:GFP-9* after 4 h of MG132 treatment (n–p), but not in the DMSO-treated control (m). MG132 treatment results in a GFP signal in both the cytoplasm (n, o) and the nucleus (n, p).
(q) Western blot analysis using anti-GFP antibodies revealing instability of the BT1:GFP and BTB:GFP fusions *in vivo*. Samples were treated for 4 h with MG132 (+) or DMSO (–). Plants overexpressing *BT1* or *GFP* were used as negative and positive controls, respectively. Note that the stability of the GFP protein in line *GFP:BT1-15* is not enhanced by MG132 treatment (black arrow head), whereas the full-length C-terminal fusions become more abundant after MG132 treatment (white arrowheads).
Scale bars: 10 μm in (a–g); 20 μm in (i, j, m–p).

et al., 2005). In addition, we found that *BT1*, *BT2* and *BT5* show a rapid and transient induction of expression by auxin (indole-3-acetic acid, IAA), at different steady-state levels, which peaks 30 min after treatment. *BT4* expression was also enhanced at this time point, but the RNA levels increased until 4 h, and enhanced levels persisted at least until 24 h after auxin treatment (Figure 3b).

Interestingly, the *bt1-4* loss of function caused a reduction of expression of the other *BT* genes in leaves, whereas it increased the expression of *BT2* and *BT5* in roots, of *BT2* in stems and flower buds, and enhanced *BT4* expression in stems. Likewise, the *bt2-3* loss of function reduced the expression of the other *BT* genes in leaves, enhanced the expression of *BT1* and *BT5* in roots, of *BT4* and *BT5* in stems and flower buds, respectively, and of both *BT4* and *BT5* in siliques, whereas *BT5* expression in seedlings and stems was significantly reduced (Figure 3a). This indicates that the genes are under reciprocal transcriptional regulation, and that a mechanism of compensational expression exists. BT proteins repress or activate the expression of alternate members in specific tissues, and *bt* loss of function results in enhanced or repressed expression of the remaining *BT* genes, which could explain the absence of phenotypes in single *bt* loss-of-function plants.

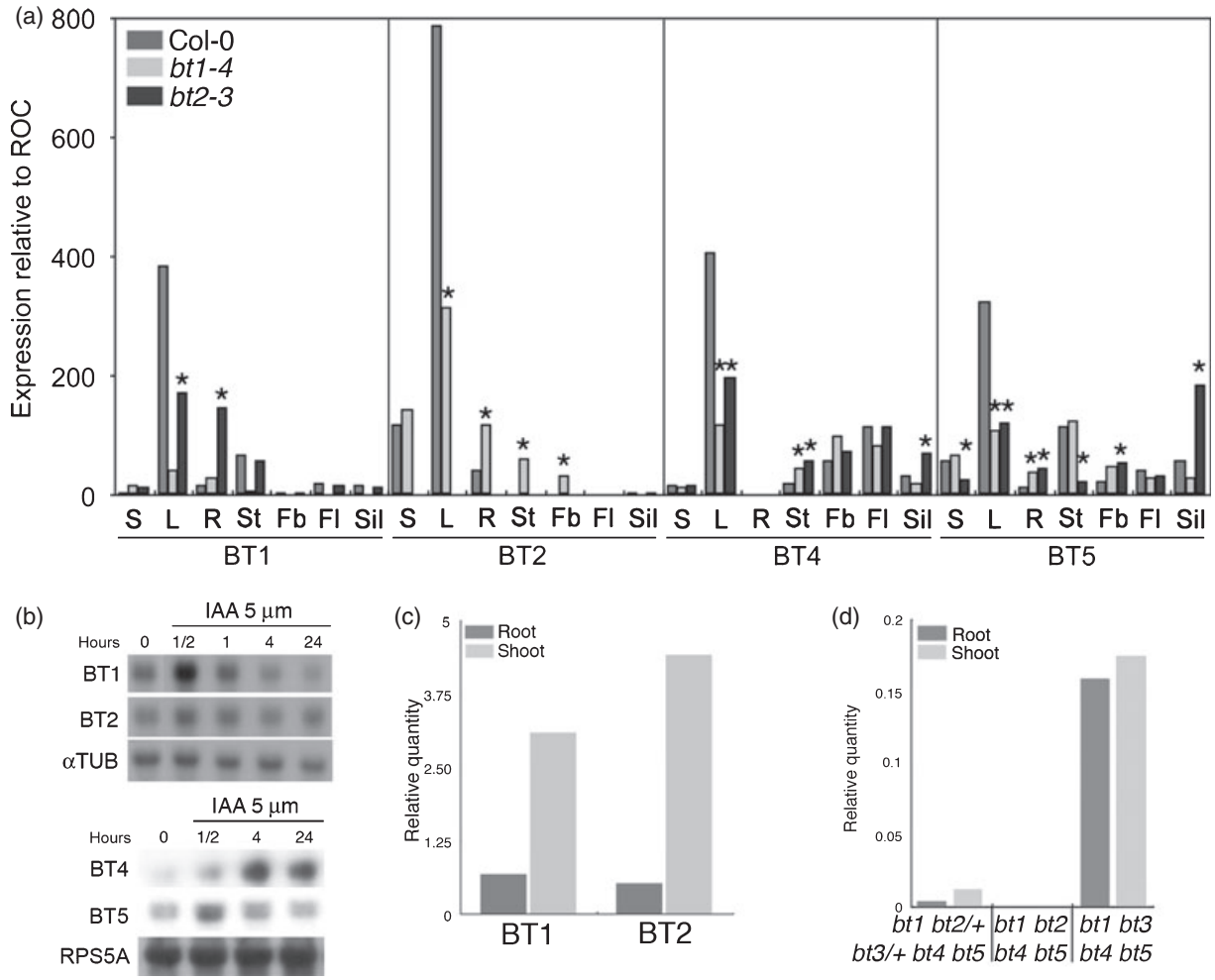

Figure 3. *BT* genes are expressed throughout plant development, and show reciprocal transcriptional regulation.
(a) Quantified northern blot analysis of the expression pattern of Arabidopsis *BT1*, *BT2*, *BT4* and *BT5* in 8-day-old seedlings (S), rosette leaves (L) and roots (R) of 3-week-old plants, or stems (St), flower buds and inflorescence meristems (Fb-M), flowers (Fl) and siliques (Sil) from 6-week-old plants of Col-0 wild type, *bt1-4* and *bt2-3*. Expression values that are more than twofold different in the mutant compared with wild type are marked with an asterisk.
(b) Northern blot analysis of *BT1*, *BT2*, *BT4* and *BT5* expression in 8-day-old seedlings after auxin (5 μM IAA) treatment for the indicated times. *α-Tubulin* and *RPS5A* were used as controls.
(c) qPCR analysis of *BT1* and *BT2* expression in roots and shoots of 10-day-old seedlings.
(d) qPCR analysis of *BT2* expression in the roots and shoots of 10-day-old seedlings in the indicated mutant backgrounds, relative to expression levels in the wild-type background.

BT1, BT2 *and* BT3 *act redundantly during gametophyte development*

As the single *bt* null mutants were wild type in appearance, mutant combinations were generated to assess the likely functional redundancy among the *BT* genes. Various combinations of double and triple mutants were indistinguishable from the wild type. However, out of the five possible quadruple mutant combinations, only *bt1 bt2 bt4 bt5* and *bt1 bt3 bt4 bt5* could be obtained as homozygous quadruple progeny, implying that quadruple mutants or gametes carrying the *bt2* and *bt3* alleles together in the homozygous state were not viable. In an attempt to identify the pentuple loss-of-function mutant, only *bt1 bt2/+bt3/+bt4 bt5* and *bt1 bt2/+bt3 bt4 bt5* plants were obtained. As *BT2* and *BT3* are located on chromosomes 3 and 1, respectively, physical linkage does not explain the absence of seedlings homozygous for both insertion alleles. In order to analyze the observed segregation distortion, the progeny of a self-pollinated *bt1 bt2/+bt3/+bt4 bt5* plant were genotyped. Neither pentuple homozygous mutants nor *bt1 bt2 bt3/+bt4 bt5* seedlings were found in over 200 genotyped seedlings. Quadruple mutants that were homozygous wild type for either *BT2* or *BT3* were obtained in a significantly higher proportion than expected (Table 1). Moreover, embryos carrying the *bt2/+bt3/+* and *bt2/+bt3* mutant combinations

Table 1 Genotypes of the progeny of a selfed *bt1 bt2/+bt3/+bt4 bt5* plant

Genotype	Observed %[a]	Expected %[b]
bt1 bt2 bt3 bt4 bt5	**0**	6.3
bt1 bt2 bt3/+ bt4 bt5	**0**	13.0
bt1 bt2 BT3 bt4 bt5	**15**	6.3
bt1 bt2/+ bt3 bt4 bt5	8	13.0
bt1 bt2/+ bt3/+ bt4 bt5	32	25.0
bt1 bt2/+ BT3 bt4 bt5	10	13.0
bt1 BT2 bt3 bt4 bt5	**25**	6.3
bt1 BT2 bt3/+ bt4 bt5	**6**	13.0
bt1 BT2 BT3 bt4 bt5	5	6.3

[a]Percentage of progeny (more than 200 seedlings) with the indicated genotype. The percentages in bold are strikingly different from the expected values.
[b]Percentage of progeny expected, based on Mendelian segregation.

did not arrest, and the resulting seedlings were indistinguishable from wild type. We therefore hypothesized that the formation or viability of gametes containing both *bt2* and *bt3* loss-of-function mutations was affected.

Genotyped F_1 progeny from reciprocal backcrosses between *bt1 bt2/+ bt3/+ bt4 bt5* and Col-0 wild type showed a segregation ratio of 2:1:1 for the gamete genotypes *BT2 BT3*:*BT2 bt3*:*bt2 BT3* ($n = 96$, $\chi^2 < 9.348$, for $P = 0.01$, in both reciprocal crosses), and the *bt2 bt3* genotype was absent from these populations. The results indicate that the *bt2* and *bt3* single and double mutations hamper gametophyte development, and lead to segregation distortion in both female and male gametogenesis (McCormick, 2004; Yadegari and Drews, 2004). However, finding *bt1 bt2/+ bt3 bt4 bt5* seedlings among 8% of the selfed progeny suggests that *bt2 bt3* double mutant gametes can occasionally escape and lead to successful seed set. Siliques of *bt1 bt2/+ bt3/+ bt4 bt5* plants showed empty spaces, characteristic of female gametophytic lethal mutations (Yadegari and Drews, 2004), whereas *bt1 bt3 bt4 bt5* siliques contained a full seed set (Figure 4a–c). Closer inspection of *bt1 bt2/+ bt3/+ bt4 bt5* siliques showed that the seed set was reduced to 30% (Figure 4c; Table 2), and that embryo and endosperm development in the set seeds was normal ($n \sim 600$; data not shown). In accordance with the reduced seed set, the siliques were almost twofold shorter for *bt2/+ bt3/+* or *bt1 bt2/+ bt3/+ bt4 bt5* plants, compared with Col-0 or *bt1 bt3 bt4 bt5* plants (Table 3). Reduced seed set and shorter siliques were also observed in *bt1 bt2/+* and *bt1 bt2/+ bt3/ +bt5* plants (Tables 2 and 3), indicating that the phenotype is strongly linked to *bt2* loss of function. Interestingly, the siliques were full in the quadruple *bt1 bt2 bt4 bt5* mutant, suggesting that in this case *BT3* is the redundant copy of *BT2*.

In a cross between *bt2* and *bt3*, 14 out of 20 F_2 plants showed the short silique and reduced seed set phenotypes (not shown). Notably, all 14 affected F_2 plants were double heterozygous for *bt2* and *bt3*, which corroborates our hypothesis that the loss of function of these two genes leads to defective gametophyte development. The six remaining wild-type-looking F_2 plants were homozygous for one of the *bt* mutations, and were homozygous the wild type for the other *BT* gene, thereby confirming that the two mutations preferably coexist in one plant when in the heterozygous state. *bt2/+ bt3/+* plants were phenotypically indistinguishable from *bt1 bt2/+ bt3/+ bt4 bt5* plants.

qPCR analysis on RNA isolated from the roots and shoots of 10-day-old seedlings showed that *BT2* expression was significantly reduced in the progeny of a *bt1 bt2/+ bt3/ + bt4 bt5* plant, compared with wild-type plants (Figure 3d), which is in line with the reduced expression observed for some *BT* genes in the leaves and stems of the *bt1-4* or *bt2-3* null mutants (Figure 3a, and see above). In *bt1 bt3 bt4 bt5* quadruple mutant plants, however, *BT2* expression was significantly enhanced, much more than could be expected based on the change from one copy to two copies of the wild-type gene, thereby corroborating the strong reciprocal expression compensation among the *BT* genes, and explaining the wild-type appearance of the *bt1 bt3 bt4 bt5* quadruple mutant plants.

Figure 4. *bt* loss of function is female gametophytic lethal.
(a–c) Siliques of a *bt2/+ bt3/+* plant (a right, b) are short and show many random empty positions (unfertilized ovules, black arrowheads in c), whereas siliques of a *bt1 bt3 bt4 bt5* plant (a left, c) show full seed set.
(d–m) Confocal sections of unfertilized female gametophytes at a mature stage (FG7), stained with propidium iodide. (d, e) Mature wild-type ovule (d) and detail of the female gametophyte (e). *bt2/+ bt3/+* ovules are either wild-type (h) or do not have an embryo sac, but instead have a fluorescent structure at the micropyle (f, g). *bt1 bt2/+ bt3/+ bt4 bt5* ovules in which the female gametophyte is completely absent, except for a fluorescent structure at the micropyle (i, j), or shows collapsed synergid cells (k) or unfused polar nuclei in the central cell (l, m).
(n–z) Megaspore development sequence in wild-type ovules stained with DAB for callose deposition (n–t), and defects observed in *bt2/+ bt3/+* ovules (u–z).
(t) Final stage of megaspore development. The degeneration of the non-selected megaspores is visible in the bright callose deposition.
(u, v) *bt2/+ bt3/+* ovules lacking megaspores showing the persistent but limited presence of callose (arrowhead). This phenotype was observed frequently (~40–60%). Note that the integuments have extended above the nucellus, even though callose persists (v).
(w, x) *bt2/+ bt3/+* ovules showing arrested megaspore development and limited callose deposition.
(y) *bt2/+ bt3/+* ovule showing callose deposition in the position normally occupied by the selected megaspore.
(z) *bt2/+ bt3/+* ovule with a relatively normal looking megaspore.
Abbreviations: EC, egg cell (long arrow); CHZ, chalaza; CSy, collapsed synergids (short arrow); D, degenerating megaspores (arrow); M, selected megaspore (arrowhead); MC, micropyle; MMC, megaspore mother cell (arrowhead); PN, polar nuclei (arrowhead); Sy, synergid cell (short arrow); UPN, unfused polar nuclei (double arrowheads). Scale bars: 20 μm.

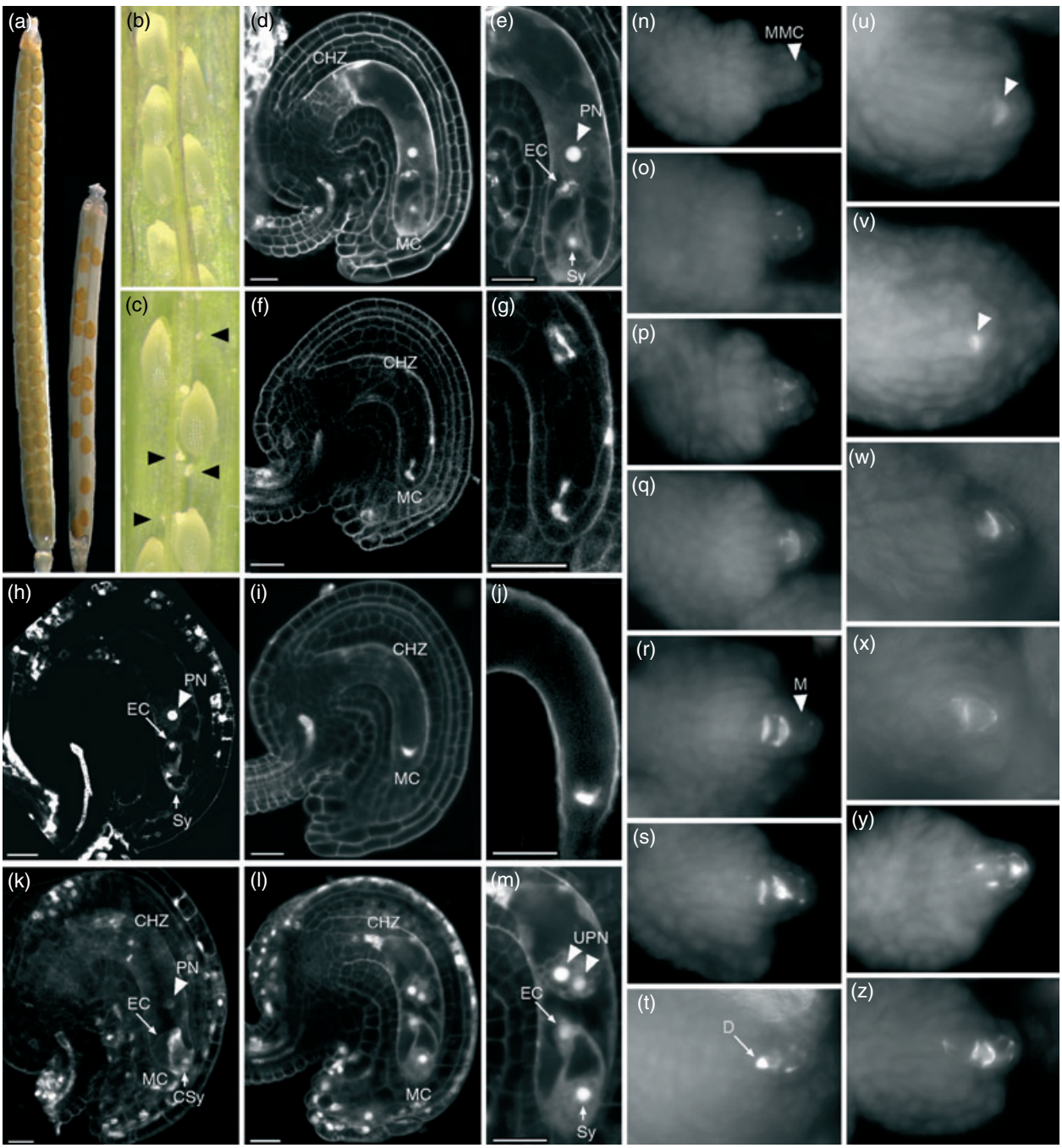

Interestingly, when we compared seed set in *bt2*, *bt1 bt2* or *bt1 bt2/+* plants, the first two genotypes showed full seed set, whereas the seed set in siliques from *bt1 bt2/+* plants was reduced to 50.1% (Table 2), which is characteristic of a single female gametophytic mutation (Yadegari and Drews, 2004). These results suggest that compensational expression by *BT3* during megagametogenesis is not sufficiently triggered in the *bt1 bt2/+* background, whereas *BT2* is haploinsufficient. *BT3* can, however, function independently in *bt1 bt2* double and *bt1 bt2 bt4 bt5* quadruple mutant plants. Therefore, the penetrances of the gametophytic lethal phenotypes in specific double, triple and quadruple combinations are jointly linked to functional redundancy and sufficient compensational expression.

Both our and previous expression studies indicate that *BT1*, *BT2* and *BT3* are expressed during gametogenesis. Firstly, our northern blot analysis and the transcriptome analysis by Hennig and co-workers (Hennig *et al.*, 2004)

Table 2 Seed set in different *bt* mutant combinations

	Seed set (%)	SD	Ovules per silique	SD	n^c
Col-0	96.5[a]	3.8	61.1	8.5	2
bt2	95.8[a]	4.1	48.8[d]	4.2	4
bt1/+bt2	92.0[a]	9.2	35.5[d]	3.8	1
bt1 bt2/+	**50.1**[a]	10.5	45.6[d]	8.6	5
bt1 bt2	98.3[a]	2.8	56.6	4.3	2
bt1 bt5	98.8[a]	1.4	47.0[d]	5.9	1
bt2/+ bt3/+	**24.8**[b]	7.8	46.8[d]	8.2	11
bt1 bt2 BT3 bt4 bt5	93.6[a]	5.7	48.0[d]	6.8	11
bt1 BT2 bt3 bt4 bt5	96.6[a]	5.2	53.2[d]	7.1	7
bt1 bt2/+ bt3/+ bt5	**31.4**[a]	10.1	40.0[d]	4.9	3
bt1 bt2/+ bt3/+ bt4 bt5	**30.0**[a]	6.0	50.2[d]	7.2	10

[a]Mean percentage of fully developed seeds per silique for four siliques per plant.
[b]Mean percentage of fully developed seeds per silique for nine siliques per plant.
[c]Number of plants tested per genotype.
[d]The number of ovules (both fertilized and non-fertilized) per silique is significantly reduced compared with Col-0 (Student's *t*-test, $P = 0.015$).

Table 3 Silique length in different *bt* mutant combinations

	Silique length (mm)[a]	SD	*n*
I			
Col	13.4	0.8	2
bt1 BT2 bt3 bt4 bt5	12.5[b]	0.6	2
bt1 bt2 BT3 bt4 bt5	12.2[b]	1.6	2
bt2/+ bt3/+	8.0[b,d]	1.1	2
bt1 bt2/+ bt3/+ bt4 bt5	8.4[b,d]	1.2	2
II			
Col	15.0	1.3	5
bt1 BT2 bt3 bt4 bt5	14.6	1.7	5
bt1 bt2/+ bt3/+ bt4 bt5	8.7[b,c]	1.6	7

[a]Mean silique length of 10 siliques per plant, *n* plants per genotype.
[b]Significantly different from Col-0 (Student's *t*-test, $P < 0.01$).
[c]Significantly different from *bt1 BT2 bt3 bt4 bt5* (Student's *t*-test, $P < 0.01$).
[d]Significantly different from *bt1 BT2 bt3 bt4 bt5* and *bt1 bt2 BT3 bt4 bt5* (Student's *t*-test, $P < 0.01$).

show that *BT1*, *BT2* and *BT3* are expressed in flower buds, where *BT2* expression is enhanced in the *bt1* mutant background (Figures S2c and S3a). Secondly, a detailed tissue profiling of all Arabidopsis *BTB* genes demonstrates that *BT1*, *BT2* and *BT3* are expressed in the pistils and stamen (Gingerich *et al.*, 2005; Figure S2b). Thirdly, gametophyte-specific microarray analyses show that both *BT2* and *BT3* are expressed at low levels in early-stage ovules (Yu *et al.*, 2005; Supplementary Figure S2d), and that *BT3* expression is tightly linked to the early steps of male gametogenesis, whereas *BT2*, *BT4* and *BT5* are expressed in mature pollen (Honys and Twell, 2004; Borges *et al.*, 2008; Figure S2e and f).

BT proteins are essential during early stages of female, and later stages of male gametophyte development

In wild type Arabidopsis, the female gametophyte develops from a diploid megaspore mother cell (MMC) that undergoes meiosis, giving rise to four haploid megaspores, from which three selected megaspores die (stage FG1). The remaining megaspore follows three rounds of mitosis to become an eight-nucleate cell (stage FG5), which, after nuclear migration and fusion, and cellularization, turns into a seven-cell structure (stage FG7; Figure 4d–e) (Christensen *et al.*, 1997; Drews and Yadegari, 2002). In unfertilized *bt2/+ bt3/+* or *bt1 bt2/+ bt3/+ bt4 bt5* ovules at the terminal stage of development (FG7) (Christensen *et al.*, 1997), a portion of the gametophytes appeared to be the same as in the wild type (17% for the pentuple mutant, $n = 42$ from two siliques; Figure 4d–e and h), whereas a significant portion of these gametophytes did not develop an embryo sac (45% for the pentuple; Figure 4f–g and i–j, respectively). Staining ovules for callose deposition with decolourized aniline blue (DAB) confirmed that the majority of *bt2/+ bt3/+* ovules lacked or displayed arrested megaspore development (Figure 4n–z), demonstrating that *bt* loss of function induces defects at the earliest stages of female gametophyte development (FG1). Additional mutant phenotypes were observed only in pentuple mutant gynoecia: gametophytes where the synergid cells had prematurely collapsed (17%; Figure 4k) and gametophytes with unfused polar nuclei (21%; Figure 4l–m). The premature synergid collapse in unfertilized ovules is an unusual phenotype, as collapse is always associated with fertilization and pollen tube arrival (Yadegari and Drews, 2004).

The effect of the *bt2* and *bt3* mutations on male gametophyte development was initially observed in cleared anthers of Col-0, *bt1 bt2 bt4 bt5*, *bt1 bt3 bt4 bt5* and *bt1 bt2/+ bt3/+ bt4 bt5* plants. In Col-0, *bt1 bt2 bt4 bt5* and *bt1 bt3 bt4 bt5* anthers, respectively, 98 ($n = 1776$), 97 ($n = 873$) and 99% ($n = 2185$) of the pollen grain are round in shape, whereas in *bt1 bt2/+ bt3/+ bt4 bt5* anthers, only 32% ($n = 1797$, Student's *t*-test, $P < 0.01$) of the pollen grains were round, and the remainder were collapsed (Figure 5a–b; data not shown). Nuclear and viability staining indicated that a portion of the *bt2/+ bt3/+* and *bt1 bt2/+ bt3/+ bt4 bt5* pollen lacked DNA, and was not viable (Figure 5c–h; data not shown). Interestingly, callose staining of tetrad microspores showed that early *bt2/+ bt3/+* tetrads had a wild-type phenotype (Figure 5i; $n = 40$ tetrads from two flowers), but that at later stages many of the *bt2/+ bt3/+* tetrads showed two collapsed microspores (Figure 5j), consistent with the segregation of a *bt2/+ bt3/+* genotype. These observations indicate that both *BT2* and

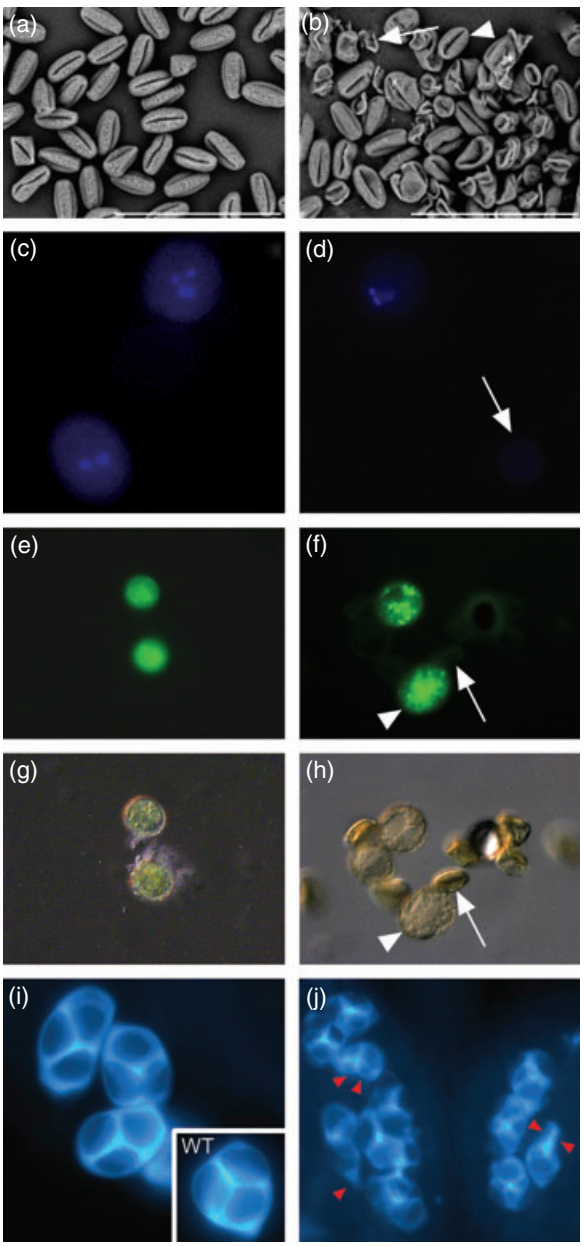

Figure 5. *bt* loss of function is male gametophytic lethal.
(a, c, e, g) Columbia and (b, d, f, h) *bt2/+ bt3/+* pollen grains.
(a, b) Scanning electron microscopy shows collapsed pollen grains segregating in *bt2/+ bt3/+* anthers.
(c, d) DAPI-stained nuclei of mature trinuclear wild-type pollen (c) and hydrated *bt2/+ bt3/+* pollen (d), some of which lack nuclei (arrow).
(e–h) FCR staining and (g, h) the corresponding DIC image, showing viable (arrowhead) and non-viable (arrow) collapsed pollen grains.
(i, j) DAB staining of *bt2/+ bt3/+* tetrads. Early tetrads (i) show little difference with wild type (inset). Late tetrads (j), many of which have double-degenerated microspores (red arrowheads).
Scale bars:100 μm.

BT3 only become essential after meiosis or subsequent cytokinesis in the microspores, which is in contrast with the role of *BT2* and *BT3* in the female gametophyte, where both genes are required for megaspore development and maturation (Figure 4u–z).

Discussion

The BTB domain proteins form a large family of scaffold proteins that are found in a wide range of organisms. Here, we studied the function of a land plant-specific subfamily, the BT proteins, in Arabidopsis, and demonstrated that there is considerable functional redundancy and transcriptional compensation among the family members. Detailed analysis of Arabidopsis plants segregating null mutations of the five *BT* genes indicated that the BT proteins perform a crucial function in plant development.

BT proteins are probably multifunctional scaffold proteins

Functional analyses of some BTB proteins in yeast and *C. elegans* indicated that these proteins are part of CULLIN3 (CUL3)-containing E3 Ubiquitin ligases (Furukawa *et al.*, 2003; Geyer *et al.*, 2003; Moon *et al.*, 2004; Pintard *et al.*, 2004), where they act as scaffolds that interact with CUL3 through the BTB domain, and select target proteins for ubiquitination through their second protein–protein interaction domain (Krek, 2003; Moon *et al.*, 2004). Members of several Arabidopsis BTB protein subfamilies, such as the NPH3 and the BTB-MATH protein families, have been found to interact with CUL3, but for the BT clade the reports are contradictory (Wang *et al.*, 2004; Dieterle *et al.*, 2005; Figueroa *et al.*, 2005; Gingerich *et al.*, 2005; Weber *et al.*, 2005). Moreover, in a yeast two-hybrid screen with BT1, we have not identified CUL3 as a BT1 interactor (Zago, 2006). Interestingly, the experiments presented here indicate that the BT1 protein itself is a target for degradation by the 26S proteasome pathway. The BT1 instability and degradation by the 26S proteasome could be part of a feedback regulation of BT1 function. Considering the variety of interacting proteins identified for the BT proteins, the presence of three protein–protein interaction domains in the structure, and the drastic effect of *bt* loss of function in Arabidopsis, it is likely that BT proteins are multifunctional scaffolds that act in, or maybe even interconnect, multiple cellular pathways.

Functional redundancy among the BT *genes*

The functional redundancy among the different Arabidopsis *BT* genes was demonstrated by expression analysis and genetic studies of the *BT* family. Both published expression data (Du and Poovaiah, 2004; Hennig *et al.*, 2004; Honys and Twell, 2004; Zimmermann *et al.*, 2004; Gingerich *et al.*, 2005; Yu *et al.*, 2005; Borges *et al.*, 2008) and our expression analysis indicated that each of the *BT* genes is expressed in a large panel of tissues, and that their respective expression

patterns overlap. Moreover, our analysis uncovered reciprocal expression compensation within the *BT* gene family. This could be through a direct effect of the BT proteins themselves on the transcription of the other *BT* family members, or by an indirect mechanism of feedback control upon *BT* expression, such as the misregulation of a negative regulator of *BT* expression. The *BT* genes were found to be auxin responsive, and given that BT proteins have been identified as interactors of PINOID (HR, MKZ, RB and RO, unpublished data), and that BT2 was found to alter auxin responses (Ren *et al.*, 2007), it is tempting to speculate that the reciprocal transcription compensation of *BT* genes is at least in part auxin-mediated.

When single *bt* mutants were crossed to obtain double, triple, quadruple or even pentuple mutant combinations, only those in which *bt2* was combined with *bt3* or *bt1* loss of function showed a reduced seed set, demonstrating that *BT2* is essential for female and male gametophyte development, and that either *BT1* or *BT3* can compensate for *bt2* null mutations. Together, our data point to a strong functional redundancy among *BT* gene family members, and indicate that BT proteins from different groups (Figure 1a) can functionally replace each other. As a result of this redundancy, the requirement of *BT* genes during gametophyte development could not be detected in the current screens for gametophyte mutants (McCormick, 2004; Yadegari and Drews, 2004).

A central role for BT2 and BT3 in gametophyte development

Our genetic analysis of Arabidopsis *bt* loss-of-function mutants indicated that the *bt2-3* and *bt3-1* null alleles can only co-occur in one plant if at least one of the genes is heterozygous for the null mutation, and that the presence of *bt2* and *bt3* nulls in the haploid mega- or microspore results in aberrant gametophyte development. *BT2 bt3* or *bt2 BT3* mega- or microspores do develop into fertile gametophytes, but at 50% of the expected frequency. Although *bt2 bt3* gametes were not detected in backcross experiments, the identification of *bt1 bt2/+ bt3 bt4 bt5* individuals among progeny from a selfed *bt1 bt2/+ bt3/+ bt4 bt5* plant (Table 1) does indicate that *bt2 bt3* spores can lead to seed set. However, a seedling homozygous for both *bt2* and *bt3* null alleles was never obtained, and the frequent early defects observed in female gametophytes of *bt2/+ bt3/+* plants suggest that the *bt2 bt3* female gametophyte is infertile.

Interestingly, among progeny of selfed *bt1 bt2/+ bt3/+ bt4 bt5* and *bt2/+ bt3/+* plants (Table 1; data not shown) we detected a two- and fourfold, respectively, over-representation of the double homozygous *bt2 BT3* and *BT2 bt3* genotypes, suggesting that gametes carrying *bt2* or *bt3* null alleles are preferred when the mother plant is heterozygous for *bt2* and *bt3*. This may relate to the observed reciprocal transcriptional regulation between *BT* genes. Possibly, the expression of *BT2* and *BT3* during gametogenesis is optimal in *bt3* or *bt2* loss-of-function backgrounds, respectively, as was shown for *BT2* in the shoots and roots of the *bt1 bt3 bt4 bt5* mutant (Figure 3d).

Analysis of female gametophytes in *bt1 bt2/+ bt3/+ bt4 bt5* plants showed gametophytes with unfused polar nuclei or with collapsed synergid cells. Unfused polar nuclei can also be found in immature gametophytes (stage FG5) and in category 4 mutants, such as *magatama1* and *magatama3*, and *gametophytic factor2* (*gfa2*) and *gfa3* (Christensen *et al.*, 1998; Shimizu and Okada, 2000; Drews and Yadegari, 2002), suggesting that such gametophytes are delayed in growth, or that their polar nuclei failed to fuse. The collapse of the synergid cells does not occur if pollination is prevented, but it is usually observed at the time of, or shortly before fertilization in wild type seeds, as a result of pollen tube penetration and the discharge of sperm cells (Faure *et al.*, 2002). Viable synergid cells are required for pollen guidance and attraction to the gametophyte for proper fertilization (Higashiyama *et al.*, 2001). The segregation distortion observed in *bt1 bt2/+ bt3/+ bt4 bt5* plants may in part be explained by a reduction of the pollen tube attraction resulting from the collapsed synergid cells in some of the gametophytes.

Together, our data suggest that the BT2 and BT3 proteins are essential during female and male gametophyte development. In fact, the *bt2 bt3* combination belongs to category 1 of female gametophytic mutations, such as *gfa4*, *gfa5*, and *female gametophyte2* and *3* (Christensen *et al.*, 1998; Drews and Yadegari, 2002), where the mutants are affected at the earliest step of the gametophyte development, and do not progress after the one-nucleus stage (FG1) (Christensen *et al.*, 1997). BT4 and BT5 are probably not involved in gametophyte development, but they may function redundantly with BT1, 2 and 3 during later steps in plant (gametophytic and vegetative) development, steps that we overlooked because of the gametophytic lethality at the early stage in the *bt2 bt3* double mutant.

Experimental procedures

Arabidopsis lines, growth conditions, transformation and protoplast transfections

The *bt1-4* (Ds transposon line GT2847), *bt2-3* (SALK_084471), *bt4-1* (SALK_045370), *bt3-1* (Flag 396E01) and *bt5-1* (GABI-Kat 771C08) alleles were obtained from CSHL (Sundaresan *et al.*, 1995), NASC (Alonso *et al.*, 2003), INRA (Samson *et al.*, 2002) and MPI (Rosso *et al.*, 2003), respectively. For detection and confirmation of the insertion, we used gene-specific primers and the insertion-specific primers LBal, Ds3-2, LB4 or GABI-LB (Table S1) for SALK, Ds transposon, FLAG or GABI-Kat lines, respectively. Arabidopsis seeds were surfaced-sterilized in 50% commercial bleach solution, and were then vernalized for 2–4 days before germination at 21°C with a 16-h photoperiod and 3000 lux on solid MA medium (Masson and Paszkowski, 1992). Plants were transferred to soil at 2- or

3-weeks-old, and were grown at 21°C with a 16-h photoperiod of 10 000 lux and at 70% relative humidity.

Protoplasts isolation from Arabidopsis Col-0 cell suspension cultures and polyethylene glycol (PEG)-mediated transfections were performed as described by Axelos *et al.* (1992) and Schirawski *et al.* (2000), with 10 μg of plasmid DNA, after which the cells were incubated for at least 16 h prior to observation.

Molecular cloning and constructs

Molecular cloning was performed following standard procedures (Sambrook *et al.*, 1989). Bacteria were grown on a LC medium containing 100 μg ml^{-1} carbenicillin (Cb) or 50 μg ml^{-1} kanamycin (Km) for *Escherichia coli* strains DH5α or Rosetta (Novagen, http://www.emdbiosciences.com/html/NVG/home.html), typical high-copy cloning plasmids or the binary vector pCambia1300, respectively, or 20 μg ml^{-1} rifampicin and 50 μg ml^{-1} Km for Agrobacterium strains containing binary vectors. Primers used during cloning procedures are listed in Table S2. The *BT1* cDNA was amplified from a cDNA batch made from Arabidopsis seedlings, using BT1_*Sal*I and BT1_*Pst*I primers, and was cloned (*Sal*I-*Pst*I) into pBluescript-SK+, giving rise to pSDM6014. The *BT2* cDNA was amplified from pUNI10183 (Yamada *et al.*, 2003) with primers BT2_*Eco*RI and BT2_*Bam*HI, and was cloned (*Eco*RI-*Bam*HI) into pUC28, to obtain pSDM6069. The *BT4* cDNA was cloned (*Stu*I-*Nco*I) from pUNI13579 (Yamada *et al.*, 2003) into pUC28, giving rise to pSDM6092. The plasmids *35S::BT1:YFP*, *35S::BT2:YFP*, *35S::BT4:YFP* and *35S::BT5:YFP* were constructed using Gateway Technology (Invitrogen, http://www.invitrogen.com), by BP recombination cloning of amplified coding regions from pSDM6014, pSDM6069, pSDM6092 and BX827434 (Castelli *et al.*, 2004), respectively, into pDONOR207, and subsequent LR recombination cloning in a pART7-derived plasmid containing the appropriate Gateway cassette in frame with a *YFP:HA* coding region (C. Galván-Ampudia, unpublished data). For *35S::BT1* (pSDM6086), the *BT1* cDNA was cloned as a *Sal*I-*Spe*I fragment from pSDM6014 into pCambia1300int-35Snos. To create *35S::GFP:BT1* (pSDM6025), the *BT1* coding sequence was cloned as a *Xho*I-*Sma*I fragment from pSDM6014 in pTH2 (Chiu *et al.*, 1996). For *35S::BT1:GFP* (pSDM6063), the *BT1* cDNA, including the start codon but excluding the stop codon, was amplified from pSDM6014 using primers M13 forward and BT1-R-minusTGA-*Sal*I. The amplified fragment was cloned as the *Sal*I fragment in pTH2 (pSDM6062). For *35S::BTB:GFP* (pSDM6066), the BTB domain containing part of BT1 was cloned as a *Nco*I fragment from pGEX-BT1 into pTH2 (pSDM6098). The N- and C-terminal *GFP* fusions were cloned (*Eco*RI-*Hin*dIII) into binary vector pCambia1300.

Northern blot analysis, RT-PCR and qPCR

Total RNA was purified using the RNeasy Plant Mini kit (Qiagen, http://www.qiagen.com). Subsequent northern blot analysis was performed as described in Memelink *et al.* (1994), using 10 μg of total RNA per sample. The following modifications were made: pre-hybridizations and hybridizations were conducted at 65°C, with 10% dextran sulfate, 1% SDS, 1 M NaCl and 50 μg ml^{-1} of single-stranded herring sperm DNA as the hybridization mix. The hybridized blots were washed for 20 min at 65°C in 2x SSPE and 0.5% SDS, and for 20 min at 42°C in 0.2x SSPE and 0.5% SDS, 0.1x SSPE and 0.5% SDS, and 0.1x SSPE, respectively. Blots were exposed to FUJI Super RX X-ray film (FUJIFILM, http://www.fujifilm.com). Probes were PCR amplified from pSDM6006 (*BT1*), pSDM6025 (*GFP*) and Col-0 genomic DNA (*BT2*, *BT4*, *BT5*, *RPS5A* and *AtROC*) using the primers listed in Table S3. PCR products were column purified (Qiagen) and radioactively labeled with [α-^{32}P]ATP (Amersham, http://www.amersham.com), using the Prime-a-gene kit (Promega, http://www.promega.com). Expression changes were quantified with GeneTools v3.07.g software (PerkinElmer, http://www.promega.com) using the TIF images from scanned autoradiograms. Values were corrected for background and then normalized to the *ROC* control.

RT-PCRs were performed as described in Weijers *et al.* (2001) using 10 μg of total RNA from 8-day-old seedlings for the RT reaction. The PCR reactions were performed using one tenth of the RT volume with the gene-specific primers (Table S3). An RT reaction with Col-0 seedling RNA, in which the reverse-transcriptase was omitted, served as a negative control.

For the qPCR, the RT reactions were performed on 2 μg of total RNA from the roots and shoots of 10-day-old seedlings using the Superscript III reverse transcriptase (Invitrogen). The qPCR reactions were carried out with 5× diluted cDNA mixtures (primers listed in Table S3) on a Bio-Rad iCycler PCR machine (Bio-Rad, http://www.bio-rad.com), using a Platinum SYBR Green qPCR SuperMix-UDG kit (Invitrogen). Data were analyzed with iCycler IQ (Bio-Rad) and qBASEplus (Biogazelle, http://www.biogazelle.com). Expression values were normalized to the *EIF4A-1* control.

Western blot analysis

Transfected protoplasts were pelleted at full speed at 4°C, resuspended in 30 μl of 1× Laemmeli sample buffer and boiled for 5 min. Half of this total protein extract was separated by SDS-PAGE (10%) using PageRuler Prestained Protein Ladder (Fermentas, http://www.fermentas.com) as a size marker. To analyze Arabidopsis lines expressing GFP-tagged BT1, total protein was extracted from 7-day-old seedlings, as previously described by Kurata *et al.* (2005). The protein concentration was determined by Bradford assay and 40 μg of protein per sample was separated by SDS-PAGE (12%). A parallel gel was run and stained with Coomassie to correct for loading differences. Gels for western blot analyses were transferred to nitrocellulose membranes (Immobilon-P; Millipore, http://www.millipore.com), which were incubated with rat horseradish peroxidase (HRP)-conjugated anti-hemagglutinin (HA) antibody (3F10, 1/2000; Roche, http://www.roche.com), or rabbit anti-GFP primary polyclonal antibody (1/5000; Molecular Probes, http://www.invitrogen.com/site/us/en/home/brands/Molecular-Probes.html) and anti-rabbit HRP-conjugated secondary antibody (1/5000; Promega). Detection followed the protocol of the Phototope-HRP Western Blot Detection Kit (New England Biolabs, http://www.neb.com).

Microscopy and phenotypic analysis

Propidium iodide (0.1 mg ml^{-1} in distilled water) was used to stain the cell walls and nuclei in roots and ovules. The female gametophyte phenotypes and GFP fusion lines were observed using 40 × dry and oil objectives on an Axioplan microscope (Zeiss, http://www.zeiss.com) equipped with a confocal laser scanning unit (MRC1024ES; Bio-Rad) and a 3CCD Sony DKC5000 digital camera (Sony, http://www.sony.com). The GFP fluorescence was monitored with a 522–532-nm bandpass emission filter (488-nm excitation). Propidium iodide was visualized using the 585-nm longpass emission filter (568-nm excitation). For the subcellular localization of the BT proteins in protoplasts, a Leica DM IRBE confocal laser scanning microscope (Leica, http://www.leica.com) was used with a 63 × water objective. The fluorescence was visualized with an

Argon laser for excitation at 514 nm, and with a 522–532-nm (YFP) emission filter. Seed set was determined in cleared siliques after treatment with a derivative of Hoyer's solution (Boisnard-Lorig *et al.*, 2001), using a Leica MZ12 stereomicroscope equipped with a 3CCD Sony DKC-5000 digital camera. Mature pollen were stained by the fluorochromatic reaction (FCR) method (Heslop-Harrison and Heslop-Harrison, 1970) or with 4′,6-diamidino-2-phenylindole (DAPI; 1 μg ml^{-1} in 7% sucrose). Immature ovules and anthers were stained in 1 DAB:1 glycerol:0.2% aniline blue, in 0.1 M K_3PO_4, pH 12 (Stone *et al.*, 1984). Observations were performed with a Zeiss AxioImager M microscope and a 40 $\times$ dry objective, and were recorded with an AxioCam camera. Images were processed in ImageJ (http://rsb.info.nih.gov/ij/) and assembled in Adobe Photoshop (http://www.adobe.com).

Acknowledgements

The authors would like to thank Gerda Lamers for helpful comments concerning microscopy, Ward de Winter for technical assistance, Pieter Ouwerkerk for providing pCambia1300int-35Snos, pCAMBIA1300 and the *35S::GFP* Arabidopsis line, the Arabidopsis Biological Resource center for providing the *BT2* and *BT4* cDNAs, and Jiri Friml for permitting HSR to conduct experiments for this manuscript in his lab. AV-S is supported by a Dutch Technology Foundation STW grant (LPB06822).

Supporting Information

Additional Supporting Information may be found in the online version of this article:

Figure S1. Northern blot analysis of the expression pattern of four of the Arabidopsis *BT* genes.

Figure S2. Data mining for the tissue-specific expression of the Arabidopsis *BT* genes.

Table S1. Primers used for the genotyping of the mutant lines.

Table S2. Primers used for cloning.

Table S3. Primers used to design northern blot probes, and used in the RT-PCR and qPCR experiments.

Please note: Wiley-Blackwell are not responsible for the content or functionality of any supporting materials supplied by the authors. Any queries (other than missing material) should be directed to the corresponding author for the article.

References

Albagli, O., Dhordain, P., Deweindt, C., Lecocq, G. and Leprince, D. (1995) The BTB/POZ domain: a new protein-protein interaction motif common to DNA- and actin-binding proteins. *Cell Growth Differ.* **6**, 1193–1198.

Alonso, J.M., Stepanova, A.N., Leisse, T.J. *et al.* (2003) Genome-wide insertional mutagenesis of *Arabidopsis thaliana*. *Science*, **301**, 653–657.

Axelos, M., Curie, C., Mazzolini, L., Bardet, C. and Lescure, B. (1992) A protocol for transient gene expression in *Arabidopsis thaliana* protoplasts isolated from cell-suspension cultures. *Plant Physiol. Biochem.* **30**, 123–128.

Bardwell, V.J. and Treisman, R. (1994) The POZ domain: a conserved protein-protein interaction motif. *Genes Dev.* **8**, 1664–1677.

Boisnard-Lorig, C., Colon-Carmona, A., Bauch, M., Hodge, S., Doerner, P., Bancharel, E., Dumas, C., Haseloff, J. and Berger, F. (2001) Dynamic analyses of the expression of the HISTONE::YFP fusion protein in *Arabidopsis* show that syncytial endosperm is divided in mitotic domains. *Plant Cell*, **13**, 495–509.

Borges, F., Gomes, G., Gardner, R., Moreno, N., McCormick, S., Feijó, J.A. and Becker, J.D. (2008) Comparative transcriptomics of *Arabidopsis* sperm cells. *Plant Physiol.* **148**, 1168–1181.

Cao, H., Glazebrook, J., Clarke, J.D., Volko, S. and Dong, X. (1997) The *Arabidopsis NPR1* gene that controls systemic acquired resistance encodes a novel protein containing ankyrin repeats. *Cell*, **88**, 57–63.

Castelli, V., Aury, J.M., Jaillon, O. *et al.* (2004) Whole genome sequence comparisons and ''full-length'' cDNA sequences: A combined approach to evaluate and improve *Arabidopsis* genome annotation. *Genome Res.* **14**, 406–413.

Chiu, W.I., Niwa, Y., Zeng, W., Hirano, T., Kobayashi, H. and Sheen, J. (1996) Engineered GFP as a vital reporter in plants. *Curr. Biol.* **6**, 325–330.

Christensen, C.A., King, E.J., Jordan, J.R. and Drews, G.N. (1997) Megagametogenesis in *Arabidopsis* wild type and the *Gf* mutant. *Sex. Plant Reprod.* **10**, 49–64.

Christensen, C.A., Subramanian, S. and Drews, G.N. (1998) Identification of gametophytic mutations affecting female gametophyte development in *Arabidopsis*. *Dev. Biol.* **202**, 136–151.

Dieterle, M., Thomann, A., Renou, J.P. *et al.* (2005) Molecular and functional characterization of Arabidopsis Cullin 3A. *Plant J.* **41**, 386–399.

Drews, G.N. and Yadegari, R. (2002) Development and function of the angiosperm female gametophyte. *Annu. Rev. Genet.* **36**, 99–124.

Du, L.Q. and Poovaiah, B.W. (2004) A novel family of Ca^{2+}/calmodulin-binding proteins involved in transcriptional regulation: interaction with fsh/Ring3 class transcription activators. *Plant Mol. Biol.* **54**, 549–569.

Faure, J.E., Rotman, N., Fortuné, P. and Dumas, C. (2002) Fertilization in *Arabidopsis thaliana* wild type: developmental stages and time course. *Plant J.* **30**, 481–488.

Figueroa, P., Gusmaroli, G., Serino, G. *et al.* (2005) Arabidopsis has two redundant CULLIN3 proteins that are essential for embryo development and that interact with RBX1 and BTB proteins to form multisubunit E3 ubiquitin ligase complexes *in vivo*. *Plant Cell*, **17**, 1180–1195.

Furukawa, M., He, Y.J., Borchers, C. and Xiong, Y. (2003) Targeting of protein ubiquitination by BTB-Cullin 3-Roc1 ubiquitin ligases. *Nat. Cell Biol.* **5**, 1001–1007.

Geyer, R., Wee, S., Anderson, S., Yates, J. and Wolf, D.A. (2003) BTB/POZ domain proteins are putative substrate adaptors for CULLIN3 ubiquitin ligases. *Mol. Cell*, **12**, 783–790.

Gingerich, D.J., Gagne, J.M., Salter, D.W., Hellmann, H., Estelle, M., Ma, L.G. and Vierstra, R.D. (2005) CULLINs 3a and 3b assemble with members of the broad complex/tramtrack/bric-a-brac (BTB) protein family to form essential ubiquitin-protein ligases (E3s) in *Arabidopsis*. *J. Biol. Chem.* **280**, 18810–18821.

Gingerich, D.J., Hanada, K., Shiu, S.H. and Vierstra, R.D. (2007) Large-scale, lineage-specific expansion of a Bric-a-Brac/Tramtrack/Broad complex ubiquitin-ligase gene family in rice. *Plant Cell*, **19**, 2329–2348.

Ha, C.M., Jun, J.H., Nam, H.G. and Fletcher, J.C. (2004) *BLADE-ON-PETIOLE1* encodes a BTB/POZ domain protein required for leaf morphogenesis in *Arabidopsis thaliana*. *Plant Cell Physiol.* **45**, 1361–1370.

Hamann, T., Benkova, E., Baurle, I., Kientz, M. and Jurgens, G. (2002) The *Arabidopsis BODENLOS* gene encodes an auxin response protein inhibiting MONOPTEROS-mediated embryo patterning. *Genes Dev.* **16**, 1610–1615.

Hellmann, H., Hobbie, L., Chapman, A., Dharmasiri, S., Dharmasiri, N., del Pozo, C., Reinhardt, D. and Estelle, M. (2003) Arabidopsis

AXR6 encodes CUL1 implicating SCF E3 ligases in auxin regulation of embryogenesis. *EMBO J.* **22**, 3314–3325.

Hennig, L., Gruissem, W., Grossniklaus, U. and Köhler, C. (2004) Transcriptome programs of early reproductive stages in *Arabidopsis*. *Plant Physiol.* **135**, 1765–1775.

Hepworth, S.R., Zhang, Y., McKim, S., Li, X. and Haughn, G.W. (2005) BLADE-ON-PETIOLE-dependent signaling controls leaf and floral patterning in *Arabidopsis*. *Plant Cell*, **17**, 1434–1448.

Heslop-Harrison, J. and Heslop-Harrison, Y. (1970) Evaluation of pollen viability by enzymatically induced fluorescence; intracellular hydrolysis of fluorescein diacetate. *Stain Technol.* **45**, 115–120.

Higashiyama, T., Yabe, S., Sasaki, N., Nishimura, Y., Miyagishima, S.y., Kuroiwa, H. and Kuroiwa, T. (2001) Pollen tube attraction by the synergid cell. *Science*, **293**, 1480–1483.

Honys, D. and Twell, D. (2004) Transcriptome analysis of haploid male gametophyte development in *Arabidopsis*. *Genome Biol.* **5**, R85.

Krek, W. (2003) BTB proteins as henchmen of Cul3-based ubiquitin ligases. *Nat. Cell Biol.* **5**, 950–951.

Kurata, T., Ishida, T., Kawabata-Awai, C. *et al.* (2005) Cell-to-cell movement of the CAPRICE protein in Arabidopsis root epidermal cell differentiation. *Development*, **132**, 5387–5398.

La Cour, T., Kiemer, L., Molgaard, A., Gupta, R., Skriver, K. and Brunak, S. (2004) Analysis and prediction of leucine-rich nuclear export signals. *Protein Eng. Design Sel.* **17**, 527–536.

Masson, J. and Paszkowski, J. (1992) The Culture response of *Arabidopsis thaliana* protoplasts is determined by the growth conditions of donor plants. *Plant J.* **2**, 829–833.

McCormick, S. (2004) Control of male gametophyte development. *Plant Cell*, **16**(Suppl), S142–S153.

Memelink, J., Swords, K.M.M., Staehelin, L.A. and Hoge, J.H.C. (1994) Southern, Northern and Western blot analysis. In *Plant Molecular Biology Manual* (Gelvin, S.B. and Schilperoort, R.A., eds). Dordrecht: Kluwer Academic Publishers, pp. 1–23.

Moon, J., Parry, G. and Estelle, M. (2004) The ubiquitin-proteasome pathway and plant development. *Plant Cell*, **16**, 3181–3195.

Motchoulski, A. and Liscum, E. (1999) Arabidopsis NPH3: An NPH1 photoreceptor-interacting protein essential for phototropism. *Science*, **286**, 961–964.

Norberg, M., Holmlund, M. and Nilsson, O. (2005) The *BLADE ON PETIOLE* genes act redundantly to control the growth and development of lateral organs. *Development*, **132**, 2203–2213.

Pintard, L., Willems, A. and Peter, M. (2004) Cullin-based ubiquitin ligases: Cul3-BTB complexes join the family. *EMBO J.* **23**, 1681–1687.

Ren, S., Mandadi, K.K., Boedeker, A.L., Rathore, K.S. and McKnight, T.D. (2007) Regulation of telomerase in *Arabidopsis* by BT2, an apparent target of TELOMERASE ACTIVATOR1. *Plant Cell*, **19**, 23–31.

Rosso, M.G., Li, Y., Strizhov, N., Reiss, B., Dekker, K. and Weisshaar, B. (2003) An *Arabidopsis thaliana* T-DNA mutagenized population (GABI-Kat) for flanking sequence tag-based reverse genetics. *Plant Mol. Biol.* **53**, 247–259.

Sambrook, J., Fritsch, F. and Maniatis, T. (1989) *Molecular Cloning - A Laboratory Manual*, 2nd edn. Cold Spring Harbor: Cold Spring Harbor Laboratory press.

Samson, F., Brunaud, V., Balzergue, S., Dubreucq, B., Lepiniec, L., Pelletier, G., Caboche, M. and Lecharny, A. (2002) FLAGdb/FST: a database of mapped flanking insertion sites (FSTs) of *Arabidopsis thaliana* T-DNA transformants. *Nucl. Acids Res.* **30**, 94–97.

Schirawski, J., Planchais, S. and Haenni, A.L. (2000) An improved protocol for the preparation of protoplasts from an established *Arabidopsis thaliana* cell suspension culture and infection with RNA of turnip yellow mosaic tymovirus: a simple and reliable method. *J. Virol. Meth.* **86**, 85–94.

Shimizu, K.K. and Okada, K. (2000) Attractive and repulsive interactions between female and male gametophytes in *Arabidopsis* pollen tube guidance. *Development*, **127**, 4511–4518.

Stogios, P., Downs, G., Jauhal, J., Nandra, S. and Prive, G. (2005) Sequence and structural analysis of BTB domain proteins. *Genome Biol.* **6**, R82.

Stone, B.A., Evans, N.A., Bonig, I. and Clarke, A.E. (1984) The application of Sirofluor, a chemically defined fluorochrome from Aniline Blue for the histochemical detection of callose. *Protoplasma*, **122**, 191–195.

Sundaresan, V., Springer, P., Volpe, T., Haward, S., Jones, J.D., Dean, C., Ma, H. and Martienssen, R. (1995) Patterns of gene action in plant development revealed by enhancer trap and gene trap transposable elements. *Genes Dev.* **9**, 1797–1810.

Tao, L.Z., Cheung, A.Y., Nibau, C. and Wu, H.M. (2005) RAC GTPases in tobacco and *Arabidopsis* mediate auxin-induced formation of proteolytically active nuclear protein bodies that contain AUX/IAA proteins. *Plant Cell*, **17**, 2369–2383.

Wang, K.L.C., Yoshida, H., Lurin, C. and Ecker, J.R. (2004) Regulation of ethylene gas biosynthesis by the *Arabidopsis* ETO1 protein. *Nature*, **428**, 945–950.

Weber, H., Bernhardt, A., Dieterle, M., Han, P., Hano, P., Mutlu, A., Estelle, M., Genschik, P. and Hellmann, H. (2005) Arabidopsis AtCUL3a and AtCUL3b form complexes with members of the BTB/POZ-MATH protein family. *Plant Physiol.* **137**, 83–93.

Weijers, D., Franke-van Dijk, M., Vencken, R.J., Quint, A., Hooykaas, P. and Offringa, R. (2001) An *Arabidopsis* Minute-like phenotype caused by a semi-dominant mutation in a *RIBOSOMAL PROTEIN S5* gene. *Development*, **128**, 4289–4299.

Yadegari, R. and Drews, G.N. (2004) Female gametophyte development. *Plant Cell*, **16**, S133–S141.

Yamada, K., Lim, J., Dale, J.M. *et al.* (2003) Empirical analysis of transcriptional activity in the *Arabidopsis* genome. *Science*, **302**, 842–846.

Yu, H.J., Hogan, P. and Sundaresan, V. (2005) Analysis of the female gametophyte transcriptome of *Arabidopsis* by comparative expression profiling. *Plant Physiol.* **139**, 1853–1869.

Zago, M.K. (2006) *Components and targets of the PINOID signaling complex in Arabidopsis thaliana*. PhD Thesis, The Netherlands: Leiden University.

Zimmermann, P., Hirsch-Hoffmann, M., Hennig, L. and Gruissem, W. (2004) GENEVESTIGATOR. Arabidopsis microarray database and analysis toolbox. *Plant Physiol.* **136**, 2621–2632.

Accession numbers: *BT1* (At5g63160), *BT2* (At3g48360), *BT3* (At1g05690), *BT4* (At5g67480), *BT5* (At4g37610), *ROC* (At4g38740), *αTubulin* (At5g44340), *RPS5A* (At3g11940), *EIF4A-1* (*AT3G13920*), *Os01g66890*, *Os01g68020*, *Os02g38320* and *Os04g40630* (Rice nipponbar *BT* genes), H0510A06.17 (rice Indica cultivar-*BT* gene), AC146856.8 (*Medicago truncatula* BT protein ABE77424), AB236807 (*Trifolium pretense* BT protein BAE71259).

GT2847 (*bt1-4*), SALK_084471 (*bt2-3*), Flag 396E01 (*bt3-1*), SALK_045370 (*bt4-1*), GABI-Kat 771C08 (*bt5-1*).

